

## Orientational order of a ferroelectric liquid crystal with small layer contraction

Rafał Korlacki,<sup>1</sup> Vitaly P. Panov,<sup>2</sup> Atsuo Fukuda,<sup>2</sup> Jagdish K. Vij,<sup>2,\*</sup> Christopher M. Spillmann,<sup>3</sup> and Jawad Naciri<sup>3</sup>  
<sup>1</sup>*Department of Physics and Astronomy and The Nebraska Center for Materials and Nanoscience, University of Nebraska–Lincoln, Lincoln, Nebraska 68588, USA*

<sup>2</sup>*Department of Electronic and Electrical Engineering, Trinity College, University of Dublin, Dublin 2, Ireland*

<sup>3</sup>*Naval Research Laboratory, Center of Bio/Molecular Science and Engineering, USA*

(Received 8 April 2010; revised manuscript received 27 July 2010; published 17 September 2010)

We present spectroscopic and optical studies of a non-layer-shrinkage ferroelectric liquid crystal DSiKN65. The orientational order parameters  $S$ , measured with respect to the smectic layer normal using IR spectroscopy on a sample aligned homeotropically, does not exhibit any significant variation between the smectic- $A^*$  and smectic- $C^*$  phases. In contrast the birefringence of a planar homogenous sample abruptly increases at the smectic- $A^*$  to smectic- $C^*$  transition. This suggests a general increase in the orientational order, which can be described by the orientational order parameters  $S'$  defined with respect to the director. Simultaneous increase of  $S'$  and the director tilt  $\Theta$  may explain the low shrinkage of smectic layers, which is consistent with recent theoretical models describing the smectic- $A^*$  to smectic- $C^*$  transition for such materials.

DOI: [10.1103/PhysRevE.82.031702](https://doi.org/10.1103/PhysRevE.82.031702)

PACS number(s): 61.30.Gd, 42.70.Df, 64.70.M–, 78.30.Jw

### I. INTRODUCTION

Discovery of ferroelectric liquid crystals (FLC) by Meyer *et al.* [1] created the basis of using new types of liquid crystal displays (LCDs). The next generation of electro-optic devices and LCDs using these fast switching materials could potentially be developed. These would have switching times of the order of a few  $\mu\text{s}$ . In order to realize such devices, however, a number of problems had to be overcome, among them was the degradation of contrast due to the so called “zigzag” defects, caused by a contraction of smectic layers at the transition from paraelectric smectic- $A^*$  ( $\text{Sm } A^*$ ) phase to tilted ferroelectric smectic- $C^*$  ( $\text{Sm } C^*$ ) phase. Therefore, some FLC materials, which were reported to exhibit a very small smectic layer shrinkage, while preserving the other typical properties of FLCs, attracted a significant attention and become an important subject of studies (see, for example, a review by Lagerwall and Giesselmann [2]).

The first to report and study this kind of FLCs was Adrian de Vries [3,4]. He proposed a model now called the “de Vries diffuse-cone” model. In his view, the molecular orientational fluctuations are represented by diffused cones within a smectic layer. The local tilting directions are correlated only within a short range for  $\text{Sm } A^*$  phase, and become correlated over the entire smectic layer at the transition to the  $\text{Sm } C^*$  phase. Thus, the transition  $\text{Sm } A^*$ - $\text{Sm } C^*$  is purely a disorder-order transition of directions of the molecular tilt fluctuations (i.e., the tilt azimuthal angles). The “diffuse-cone model” explains why the smectic layer spacing may become preserved during the  $\text{Sm } A^*$ - $\text{Sm } C^*$  transition, but the structure of  $\text{Sm } A^*$  phase of “de Vries”-like materials is then qualitatively different from that of “ordinary” FLCs, for which the  $\text{Sm } A^*$  phase is often referred as “orthogonal.” Moreover, it is somewhat confusing that de Vries, introducing his diffuse-cone model did not actually use the term ‘director’, which is the principal way of defining various liquid crystal phases. It

is therefore natural to ask: Is the director in de Vries  $\text{Sm } A^*$  phase tilted from the smectic layer normal, at least locally, or not? If the answer is yes, then de Vries  $\text{Sm } A^*$  phase should actually belong to the  $\text{Sm } C$  family, not  $\text{Sm } A$ , as has been proposed by Meyer and Pelcovits [5].

If the director is not tilted in the ‘de Vries’  $\text{Sm } A$ , the question is how to draw a line between the two  $\text{Sm } A$  phases and what is the origin of their differences? In other words: Do we really need to consider two different scenarios for the  $\text{Sm } A^*$ - $\text{Sm } C^*$  phase transition? How might it be possible that essentially the same phase transition needs different description (perhaps even a different order parameter) for various materials? Is it then possible to create a model describing all such phenomena consistently? All these questions seem to be recently answered by theoretical efforts by Saunders *et al.* [6], Gorkunov *et al.* [7], and Osipov *et al.* [8]. These theories reproduce various transition scenarios and have several common features. For example, a small shrinkage of smectic layers at the  $\text{Sm } A$  to  $\text{Sm } C$  phase transition requires an exceptionally small orientational order in the  $\text{Sm } A$  phase, and qualitatively the same shape of the molecular distribution function in  $\text{Sm } A$  phase does not support de Vries “diffuse-cone” picture. In particular, in models by Gorkunov *et al.* [7] and Osipov *et al.* [8] the uniaxial order parameter,  $S'$  in our notation, is strongly temperature dependent and its rapid increase at the  $\text{Sm } A$  to  $\text{Sm } C^*$  phase transition compensates the effect of the director tilt on the layer spacing. As we will show later, the necessary condition, an exceptionally small value of the parameter  $S'$  in the  $\text{Sm } A$  phase seems indeed to be a common feature of the de Vries materials.

The theoretical approach used by Osipov *et al.* [8] and Gorkunov *et al.* [7] relies on the formalism of orientational order parameters, which to some extent are the same as these that can be extracted experimentally using IR spectroscopy. It is our intention, therefore, in this paper to present experimental data that can be compared with predictions of their theory.

### II. EXPERIMENT

Material used in this study was DSiKN65 [Fig. 1(a)], which together with its homolog, TSiKN65, is considered

---

\*Author to whom correspondence should be addressed; [jvij@tcd.ie](mailto:jvij@tcd.ie)

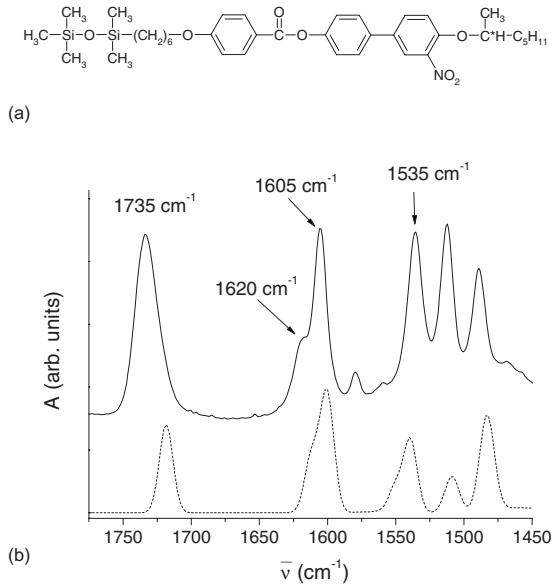


FIG. 1. Molecular structure of DSiKN65 (a) and a region of its IR spectrum of stretching vibrations well-localized within the molecular core (as listed in Table I); solid line-experimental spectrum, dashed line-theoretical spectrum obtained using the density functional theory (for details see the text).

typical de Vries compounds [9–12]. The latter one was studied even more often, but DSiKN65 is more convenient, as temperatures of its phase transitions are not as close to ambient temperatures. Both homologs possess essentially the same properties, so our conclusions are applicable to both of them. We investigated a sample cell aligned homeotropically, which is a sample geometry especially suitable in this case. The IR beam is always parallel to the smectic layer normal, and the experiment using nonpolarized IR beam on a multidomain sample with the smectic helical structure present is sensitive primarily to the tilt, but not to variations of tilting directions (see Korlacki *et al.* [13]). Therefore, for a hypothetical sample perfectly holding the pure de Vries scenario one should not expect any differences in IR spectra between Sm  $A^*$  and Sm  $C^*$  phases. In order to perform infrared (IR) studies the sample was sandwiched between two ZnSe windows covered by chromolane (Aurat Joint Co., Moscow, Russia) layers for obtaining the homeotropic orientation and with mylar spacers 5 microns thick. The layers of chromolane were obtained by spin-coating from a 0.5% solution in propanol-2, and cured for 0.5 h in 120 °C. The sample cell was filled in a temperature just above the transition to the isotropic phase. IR spectra were recorded using Bio-Rad FTS-6000 Fourier Transform IR spectrometer, with a temperature step 0.3 °C on cooling from the isotropic phase, with an accumulation over 32 scans per point. For each experimental point the temperature was stabilized for 300 s prior to acquiring the spectra. Absorption bands chosen for further analysis were fitted using a numerical approximation of Voigt function. In order to confirm the assignments of the IR bands, and to obtain a detailed information on IR transition dipole moments we performed molecular modeling using a commercial package PQS [14] (the density functional theory (DFT) method-hybrid functional B3LYP [15,16] and

TABLE I. Infrared bands discussed in the paper and shown in Fig. 1(b), and orientations of their transition dipole moments as a polar angle  $\beta$  between the long molecular axis and the vector of transition dipole moment (TDM).

Frequency (cm <sup>-1</sup> )	IR mode	TDM $\beta$ (deg)
1735	Carbonyl (C=O) stretching	65
1620	Nitrophenyl ring (C—C) stretching	17
1605	Phenyl ring (C—C) stretching	8
1535	Nitryl (NO <sub>2</sub> ) stretching	37

split-valence basis set with polarized [17,18] and diffuse [19] functions 6-31+G<sup>\*</sup>). The obtained force field was then scaled with the scaled quantum mechanical (SQM) procedure [20–22] using the transferable set of scaling factors given in Ref. [21]. A list of major IR bands and orientations of their transition dipole moments are given in Table I.

The birefringence measurements were made on a sample prepared in a planar cell fabricated by Citizen Co., Japan with Nissan RN-1266 polyimide alignment layer of thickness 1.3  $\mu\text{m}$ , with rubbing on only one of the substrates, and filled with the sample in the isotropic phase using the capillary method. The small cell thickness suppressed the formation of a smectic helical structure in the Sm  $C^*$  phase. For this experiment we used a photoelastic modulator based system (HINDS PEM-90, I/FS50 optical head; National Instruments USB data acquisition board), which allows accurate measurements of the sample retardation  $\Gamma$ . The birefringence can be determined as  $\Delta n = \Gamma \lambda / \pi d$ , where  $d$  is the thickness of the cell and  $\lambda$  is the wavelength of the light source [in our case red light emitting diode with a corresponding  $\lambda = 632.8$  nm narrow-band (10 nm bandwidth) optical filter]. Our microscope based PEM system acquires a throughput of light from an area of approximately 200  $\times$  200 micrometers of the cell, and the sample was cooled at a rate of 0.2 °C/min throughout the experiment.

X-ray measurements were performed using Cu K $\alpha$  radiation and a Bruker Platinum-135 charge-coupled device (CCD) detector on a MicroSTAR-H generator equipped with Helios optics. A bulk sample of DSiKN65 on a microscope cover glass was mounted in a temperature controlled stage connected to an Instec control unit (STC200G, Instec, Inc., Boulder, CO). The stage was positioned with a stand such that the cover glass was normal with respect to the incident radiation. Diffraction images of the primary layer spacing were collected in one or two degree temperature increments and the sample was allowed to equilibrate for a minimum of eight minutes at each temperature. The sample was first heated, then cooled through the Sm  $A^*$ -Sm  $C^*$  transition and the primary layer spacing analyzed (only values for the cooling cycle shown). For each diffraction image collected at a given temperature, an annulus of the scattering intensity corresponding to the primary layer spacing was plotted as a function of the solid cone angle,  $2\theta$ . A linear correction was applied to subtract background scattering. Next, a least-squares fit to a Gaussian line shape was used to determine the center of the primary smectic layer spacing at each temperature.

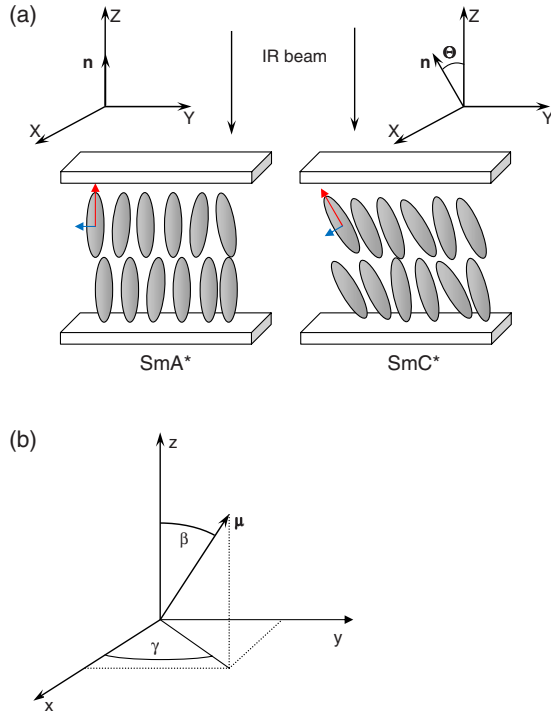


FIG. 2. (Color online) (a) Schematic of the experimental arrangement. Orientation of the director  $\mathbf{n}$  in the laboratory reference system  $XYZ$  shown for two typical phases:  $\text{Sm } A^*$  and  $\text{Sm } C^*$ . Arrows indicate the direction of the IR beam. Please, note that the IR beam is not polarized, hence the tilting direction (the azimuthal angle) of the director does not matter. Also shown example IR transition dipole moments parallel and perpendicular to the long molecular axis. (b) Definitions of angular coordinates  $\beta$  and  $\gamma$  specifying the orientation of an IR transition dipole moment  $\mu$  in the molecular reference system  $xyz$ . For details see the text.

### III. RESULTS AND DISCUSSION

Let us now explain how the IR absorbance  $A$  allows us to obtain the orientational order parameters (for details see Ref. [13]). For an LC sample aligned homeotropically and being in the  $\text{Sm } A$  phase the director is parallel to the smectic layer normal and to the IR beam (see Fig. 2). Thus, the electric vector of a nonpolarized IR beam probes the projection of the IR transition dipole moments onto the smectic layer plane ( $XY$ -plane in the laboratory reference system). For a given IR band the IR absorbance normalized with respect to the isotropic phase is a function of the orientational order parameters  $S$  and  $D$  [23,24],

$$A = (A_X + A_Y)/A_0 = 1 - S \cdot P_2(\cos \beta) - \frac{1}{2}D \cdot \sin^2 \beta \cos 2\gamma, \quad (1)$$

where  $P_2(\cos \beta)$  is second Legendre polynomial  $P_2(x) = \frac{1}{2}(3x^2 - 1)$ ,  $A_0$  is the isotropic component of the IR absorbance (i.e., the IR absorbance in the Isotropic phase).  $\beta$  and  $\gamma$  are Euler angles describing the orientation of the vector of IR transition dipole moment in the molecular reference system. The orientational order parameters  $S$  and  $D$  describe the uniaxial and biaxial ordering, respectively, or in other words,

the tendency of long and short molecular axes to orient along a preferred direction (in case of the long axes this direction is the line parallel to the smectic layer normal; in case of the short axes the direction may be chosen arbitrarily as the origin for  $\gamma$ ). For a band, which is well parallel to the long molecular axis we can neglect the term proportional to  $\sin^2 \beta$  (approximation of small  $\beta$ ) and the orientational order parameter  $S$  is given by a simple relation [note that when  $\beta \rightarrow 0$ , then  $P_2(\cos \beta) \rightarrow 1$ ],

$$S = \frac{1 - A}{P_2(\cos \beta)}. \quad (2)$$

In any tilted  $\text{Sm } C$  phase the director is inclined from the layer normal by  $\Theta$ . The projections of parallel IR transition dipole moments onto the smectic layer plane become larger, and consequently the values of  $S$  obtained using the equations above become smaller. It is therefore convenient to introduce an additional reference system connected with the local director. The uniaxial order parameter  $S'$  in this new local frame of reference are insensitive to changes of  $\Theta$ , and the relationship between  $S$  and  $S'$  is [13,25]

$$S = S' P_2(\cos \Theta). \quad (3)$$

$S$  is a measure of the orientational order with respect to the layer normal and is identical to  $S_k$  in theoretical description by Gorkunov *et al.* [7] and Osipov *et al.* [8],  $S'$  on the other hand reflects directly the uniaxial order, i.e., always increases as the temperature fluctuations decrease on cooling. In the  $\text{Sm } A$  phase  $S = S'$  (in the discussion below in all parts applicable to  $\text{Sm } A^*$  phase only we will use them alternatively depending on the context). The main idea of Gorkunov *et al.* [7] and Osipov *et al.* [8] is that nonlayer shrinkage is caused by  $S$  being constant, because  $S'$  and  $\Theta$  increase simultaneously.

The values of the orientational order parameters  $S'$  determined using the parallel IR band at  $1605 \text{ cm}^{-1}$  (Fig. 3) hardly show any variation between  $\text{Sm } A^*$  and  $\text{Sm } C^*$ . It is not unexpected hence we are dealing with a non-layer-shrinkage material, and it has been observed previously that there is a close relationship between  $S$  and the smectic layer thickness  $d$  [7,27,28] (see Fig. 4),

$$d = \frac{S + 2}{3}l, \quad (4)$$

where  $l$  is the molecular length, and  $d = l$  in the limit of  $S$  equal 1. Also, the obtained values of the parameter  $S$  in  $\text{Sm } A^*$  (0.49) are much lower than what would be considered "typical" for an FLC ( $S \approx 0.7$ , see for example Ref. [29]). This value is certainly among the lowest values of  $S$  ever reported for an FLC. This information alone may be interpreted in one of the two possible ways:

(i) The molecules are considerably tilted in both,  $\text{Sm } A^*$  and  $\text{Sm } C^*$ , and this reduces the value of  $S$  determined with respect to the smectic layer normal according to Eq. (3). In other words we can accept the de Vries scenario here.

(ii) The orientational order parameter  $S'$  is just very small in  $\text{Sm } A^*$ , but increases rapidly in  $\text{Sm } C^*$ , as predicted by Gorkunov *et al.* [7]

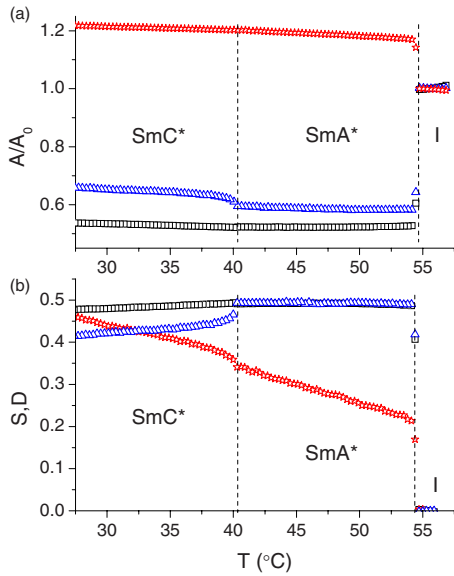


FIG. 3. (Color online) (a) IR absorbance normalized with respect to the isotropic phase vs temperature for three absorption bands; squares-phenyl ring stretching 1605  $\text{cm}^{-1}$ , triangles-nitrophenyl ring stretching 1620  $\text{cm}^{-1}$ , red stars-carbonyl stretching 1735  $\text{cm}^{-1}$  (b) Orientational order parameters vs temperature; squares- $S$  determined using band 1605  $\text{cm}^{-1}$ , triangles- $S$  determined using band 1620  $\text{cm}^{-1}$ , red stars- $D$ . Note that in the range of Sm A\* phase  $S=S'$ .

The difference between the two scenarios may appear very subtle at first, but the difference between the orientational distributions is quite significant (see Fig. 5). De Vries’ diffuse-cone model assumes that the molecules are oriented at a preferred angle with respect to the smectic layer normal. In the ideal case (pure de Vries’ scenario) this angle is the same as the director tilt angle in Sm C\* phase and only the azimuthal angles of the molecules orient during the Sm A\*-Sm C\* transition. In case of a conventional Sm A\* distribution with a very low orientational order, many molecules are tilted from the smectic layer normal by fairly large angles, and this is clearly a common feature of these two models. The difference in the shape of the distribution close

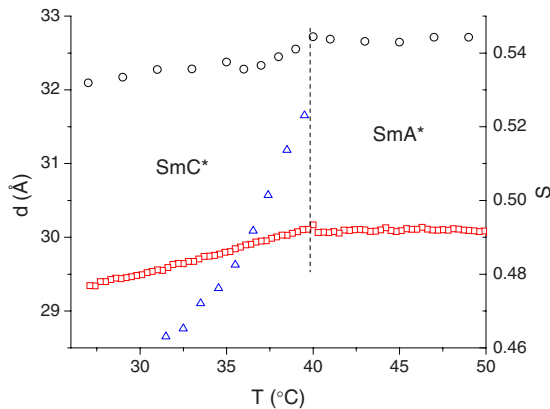


FIG. 4. (Color online) Smectic layer spacing  $d$  vs temperature: measured on cooling (circles), expected from the optical tilt (triangles); orientational order parameter  $S$  (squares).

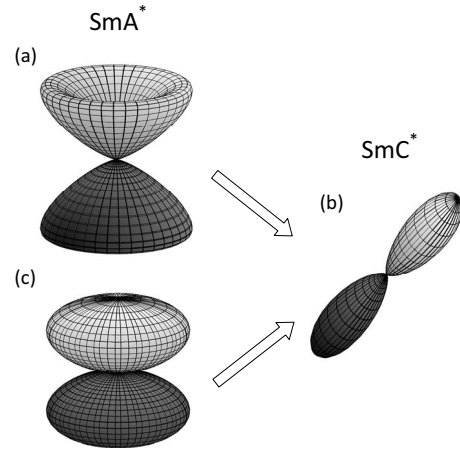


FIG. 5. Two alternative transition scenarios (represented by arrows) from Sm A\* to Sm C\* phase shown in terms of changes in the orientational distribution functions with polar and azimuthal angles in a single layer. The upper part represents the pure de Vries scenario and shows the corresponding diffuse-cone distribution of molecules in the Sm A\* phase (a) (see also Lagerwall *et al.* [26]). The transition to Sm C\* phase (b) proceeds as ordering of the azimuthal angles of molecules. In the lower part of the figure, the orientational distribution in the Sm A\* phase is conventional (c), but very broad (with very low orientational order,  $S=0.5$ ). Following the transition to Sm C\* phase the director tilts and the orientational order increases. For details on the distribution functions see the Appendix.

to the layer normal, however, is too substantial to be neglected.

In order to try to distinguish between these two scenarios we need to find additional piece of evidence. A hint as to which scenario should be favored is the temperature dependence of  $S$  determined using the IR band at 1620  $\text{cm}^{-1}$ . Values of  $S$  obtained using both, 1605 and 1620  $\text{cm}^{-1}$ , show perfect agreement within the range of Sm A\* phase [which means that the angle between the transition dipole moments for these two modes obtained using DFT, 9°, is rather correct—in contrast the values of IR absorbance in Fig. 3(a) are quite different]. In Sm C\* phase, however, the values of  $S$  obtained using the vibrational band of nitrophenyl decrease, which according to Eq. (3) is a clear signature of tilting of the director (see also Ref. [13]).

An additional evidence in favor of the model by Gorkunov *et al.* [7] and Osipov *et al.* [8] is provided by optical measurements. The sample birefringence (Fig. 6) measured without an external field, shows an abrupt increase at the Sm C\*-Sm A\* transition (by 36%, which compares with a 43% increase for the analog material, TSiKN65 [12]). The best and simplest explanation of this behavior is a large increase of the uniaxial orientational order, i.e.,  $S'$ . Let us make a brief calculation at this point. From Eq. (3) we can calculate  $S'$  knowing values of  $S$  and  $\Theta$ . Optical tilt data for DSiKN65 were published by Naciri *et al.* [9], and  $\Theta$  saturates at about 32° at the temperature 15° below the Sm A\*-Sm C\* phase transition. We can then calculate that  $S'$  saturates at 0.8—a value, which is very typical for the Sm C\* phase [29]. If we now assume that the birefringence depends primarily on  $S'$ , and we can neglect all other contributions, we can use a simple equation:  $\Delta n=B \cdot S'$ , where  $B$  is a con-



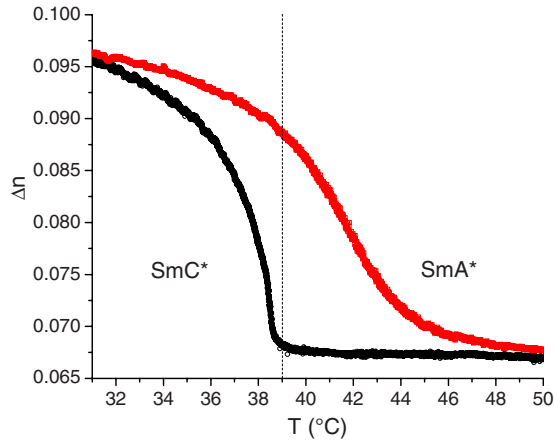


FIG. 6. (Color online) Birefringence of DSiKN65 vs temperature. Lower curve (circles)—without an external field, upper curve (squares)—with a  $5 \text{ V}/\mu\text{m}$  bias. Helix is mostly unwound by surfaces in  $\text{Sm} C^*$  phase in the absence of external field.

stant fitted to the experimental values so that  $S' = S$  in  $\text{Sm} A^*$  reproduces  $\Delta n$  in the same temperature range. Then the increase of  $S'$  to 0.8 corresponds to an increase of birefringence to 0.11. Considering that the values of birefringence we actually measure in  $\text{Sm} C^*$  phase are probably slightly lowered by relics of the smectic helical structure, there is good agreement between this expected value and our measurements.

Let us now check what we can learn from the molecular biaxial order parameter  $D$ . In order to determine it we need one perpendicular vibration (i.e., with  $\beta$  higher than the “magic angle”  $54.7^\circ$ ). The carbonyl stretching is a good candidate, as there is only one such group in the molecular structure, so its transition dipole moment is also well localized. We determine the parameter  $D$  from Eq. (1) using the previously obtained values of  $S$  (for the band  $1620 \text{ cm}^{-1}$ ), and its values are given in Fig. 3.

The orientational order parameter  $D$  is defined [23] as a difference of probabilities of finding the molecular axes  $x$  and  $y$  along the laboratory axis  $Z$ . Its value reflects the degree of order of short molecular axes, and hence also the degree of order of transversal components of the dipole moment, and hence it couples to the spontaneous polarization [8]. We note here that the values of  $D$  we obtained are much larger than reported before for an FLC [30] and are quite significant already in the  $\text{Sm} A^*$  phase. This is not surprising as the general low value of  $S$  in  $\text{Sm} A^*$  means that many molecules are significantly tilted from the smectic layer normal, which gives rise to the high molecular biaxiality. Such a tendency: low  $S$ -high  $D$  has been observed before for uniaxial phases (nematic and smectic-A) and molecular field theories of these phases predict  $D$  to be highest for  $S \approx 0.5$  [31,32]. In case of FLCs, the studies of molecular biaxiality, because of its importance in the creation of the spontaneous polarization, have already certain history (see for example Refs. [33–36]), yet, very few studies provide actual values of the parameter  $D$ . For the purpose of this story we note that a rather high value of  $D$  means that there does exist a strong tendency to orient molecular dipoles and we should expect a rather strong response to an external field already in the

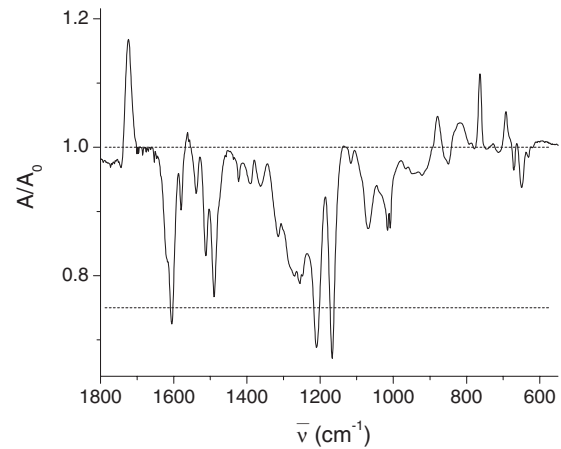


FIG. 7. IR spectrum of DSiKN65 in  $\text{Sm} A^*$  phase ( $53^\circ \text{C}$ ), divided by a spectrum in isotropic phase. Parallel bands ( $\beta < 54.7^\circ$ ) point down, perpendicular bands point up. The lower values of  $A/A_0$ , reflect the closeness on average of the transition dipole moments to the smectic layer normal.

paraelectric  $\text{Sm} A^*$  phase. This is known as the electroclinic effect, and is visible for example in the temperature dependence of birefringence with an external bias field (Fig. 6). A large electroclinic effect is a signature of deVries  $\text{Sm} A^*$  phase, but it seems it could be explained in terms of the molecular biaxial order parameter without involving the actual de Vries’ molecular distribution.

The experimental evidence presented above essentially shows that at the phase transition  $\text{Sm} A^* - \text{Sm} C^*$  there is an increase of both,  $S'$  and  $\Theta$ . Now we would like to check what happens at the Isotropic- $\text{Sm} A^*$  transition, i.e., if the sample develops some partial tilt early in the  $\text{Sm} A^*$  phase, as it would be expected for the de Vries  $\text{Sm} A^*$ , or if this is an ordinary  $\text{Sm} A^*$  phase, just disordered. In other words we would like to verify if we deal with a pure scenario, of either of the two listed above, or some mixing of them. We can try to detect tilting of molecules by looking at the entire IR spectrum for a band, for which the vector of the IR transition dipole moment is on average oriented closest to the smectic layer normal, for example closer than the CC stretching modes we analyzed above. (It is worth noting here that the molecular structure of DSiKN65 makes its IR spectrum exceptionally rich in bands that are not perfectly parallel or perpendicular.) For such a band, the average projection of the IR transition dipole moment on the smectic plane should be rather low, therefore we may expect a large drop of absorbance at the transition from the Isotropic to the  $\text{Sm} A^*$  phase, i.e., a low value of the absorbance dichroic ratio.

Figure 7 shows a plot of the IR dichroic ratio between the Isotropic and  $\text{Sm} A^*$  phase. The plot was obtained by dividing a complete IR spectrum taken in  $\text{Sm} A^*$  phase, just below the transition from the isotropic phase, by a spectrum taken just above the transition. There are only three IR bands with the IR dichroism less than 0.75. (Please note that in this procedure—dividing two spectra point by point—we compare amplitudes of the peaks rather than their areas, so the values we obtain are different than values of  $S$  shown in Fig. 3.) One of them is our reference band—phenyl ring CC

TABLE II. Uniaxial order parameters  $S$  in  $\text{Sm } A^*$  phase for chosen ferroelectric and antiferroelectric liquid crystals. The values shown were all obtained using the aromatic CC stretching band about  $1600 \text{ cm}^{-1}$  according to a uniform procedure and samples aligned homeotropically as in the current paper, and picked from the middle of the temperature range of  $\text{Sm } A^*$  phase for each material.

Material	$S$	Source
MHPOBC	0.73	[28]
TFMHPNCBC	0.65	[28]
12OF1M7	0.61	[13]
MC513	0.55	[37]
4FH6-A (OAFCL)	0.51	[37]
DSiKN65	0.49	

stretching ( $1605 \text{ cm}^{-1}$ ). The other two are bands at  $1167 \text{ cm}^{-1}$  (phenyl ring CH in-plane deformation) and  $1209 \text{ cm}^{-1}$  (COC stretching). They are well known to be parallel to the molecular long axis, actually they are even more parallel than CC stretching (their angles  $\beta$ , calculated theoretically are for both of them just a few degrees, while for  $1605 \text{ cm}^{-1}$  there are two vectors with  $\beta \approx 7^\circ$  and  $10^\circ$ , respectively), although not as convenient as they are usually accompanied by other bands and hard to extract from their neighborhood. If we used one of those bands for our calculations of the order parameters we should expect to obtain slightly higher values of  $S$ , but in any case we may conclude that there is no evidence that the molecular long axes are on average tilted from the smectic layer normal.

Finally, we would like to point out that the values of the orientational order parameters presented in this paper, although not typical, are not unique. Table II shows values of  $S$  in the  $\text{Sm } A^*$  phase for a number of ferroelectric and antiferroelectric liquid crystals, and it seems that they span a very broad range of values quite uniformly. These of the materials listed in Table II, which have their values of  $S < 0.6$ , were reported as either electroclinic or deVries materials in the past. It seems, therefore, that there do exist a good correlation between these two factors. But it also means that we should probably stop speaking about typical values of the orientational order parameters, at least in the case of  $\text{Sm } A^*$  phase.

#### IV. CONCLUSIONS

We have shown, for a typical de Vries-like FLC that this material exhibits values of the orientational order parameters substantially different than those commonly considered as “typical.” By comparing spectroscopic and optical data we can conclude that the uniaxial order parameter  $S'$ , low in the  $\text{Sm } A^*$  phase, strongly increases below the  $\text{Sm } A^*$ - $\text{Sm } C^*$  phase transition. Our results on the whole are thus perfectly consistent with the theoretical model by Gorkunov *et al.* [7] and Osipov *et al.* [8], and these models are sufficient to ex-

plain all experimental facts, also for materials with very low layer contraction. Hence, on the basis of the Occam’s razor and lacking any hard experimental evidence to the contrary, there is no need to consider the diffuse-cone model by deVries anymore.

#### ACKNOWLEDGMENTS

Authors would like to thank John H. Konnert for his help in the diffraction data analysis. Parts of this work were supported by the Science Foundation Ireland, EU network SAMPA, U.S. Department of Energy (EPSCoR, Grant No. DE-FG02-08ER46498) and the Nebraska Research Initiative.

#### APPENDIX: ORIENTATIONAL DISTRIBUTION FUNCTIONS

In order to draw to orientational distribution functions we used the angular part of the McMillan orientational distribution for the  $\text{Sm } A^*$  phase [38,39]:

$$f(\theta) = \frac{\exp\left(\frac{P_2(\cos \theta)}{\sigma}\right)}{\int_0^\pi \exp\left(\frac{P_2(\cos \theta)}{\sigma}\right) \sin \theta d\theta}, \quad (\text{A1})$$

and plotted it in three dimensions in ordinary spherical coordinates  $\theta, \varphi$ , where  $\theta$  and  $\varphi$  are polar and azimuthal coordinate, respectively. The function defined above describes the conventional orientational distribution in the  $\text{Sm } A^*$  phase. We obtained the de Vries’ “diffuse-cone” distribution as  $f(\theta - \pi/6)$ . For the  $\text{Sm } C^*$  phase we plotted the conventional distribution rotated by  $\pi/6$ . (Thus we neglect the biaxiality of the orientational distribution in tilted smectic phases, but the current story is focused mainly on the  $\text{Sm } A^*$  phase, and we do not intend to discuss properties of other phases in much detail.)

This is worth noting here that a properly normalized molecular distribution function is in fact a probability density of finding a molecule at a given orientation. Therefore, we can use it to numerically estimate average values, for example

$$S = \langle P_2(\cos \theta) \rangle = \int_0^\pi P_2(\cos \theta) f(\theta) \sin \theta d\theta. \quad (\text{A2})$$

We adjusted the width parameter  $\sigma$  in Eq. (A1) in such a way that the uniaxial orientational order parameter with respect to the layer normal  $S=0.5$  for all three distributions, and  $S'=0.8$  in the  $\text{Sm } C^*$  phase. It turns out that for such distributions the smectic layer spacing (the average projection of molecules onto the smectic layer normal) is approximately the same, 82% of the molecular length for both alternative distributions for the  $\text{Sm } A^*$  phase, and 81% of the molecular length for the  $\text{Sm } C^*$  phase.

The plots of the distribution functions shown in Fig. 5 were prepared using Mathcad ver. 13 (Mathsoft, Inc.).

- [1] R. B. Meyer, L. Liébert, L. Strzelecki, and P. Keller, *J. Physique Lett.* **36**, 69 (1975).
- [2] J. P. F. Lagerwall and F. Giesselmann, *ChemPhysChem* **7**, 20 (2006).
- [3] A. de Vries, *J. Chem. Phys.* **71**, 25 (1979).
- [4] A. de Vries, A. Ekachai, and N. Spielberg, *Mol. Cryst. Liq. Cryst. Lett.* **49**, 143 (1979).
- [5] R. B. Meyer and R. A. Pelcovits, *Phys. Rev. E* **65**, 061704 (2002).
- [6] K. Saunders, D. Hernandez, S. Pearson, and J. Toner, *Phys. Rev. Lett.* **98**, 197801 (2007).
- [7] M. V. Gorkunov, M. A. Osipov, J. P. F. Lagerwall, and F. Giesselmann, *Phys. Rev. E* **76**, 051706 (2007).
- [8] M. A. Osipov, M. V. Gorkunov, H. F. Gleeson, and S. Jaradat, *Eur. Phys. J. E* **26**, 395 (2008).
- [9] J. Naciri, J. Ruth, G. Crawford, R. Shashidar, and B. R. Ratna, *Chem. Mater.* **7**, 1397 (1995).
- [10] J. V. Selinger, P. J. Collings, and R. Shashidhar, *Phys. Rev. E* **64**, 061705 (2001).
- [11] P. J. Collings, B. R. Ratna, and R. Shashidhar, *Phys. Rev. E* **67**, 021705 (2003).
- [12] U. Manna, J.-K. Song, J. K. Vij, and J. Naciri, *Appl. Phys. Lett.* **94**, 012901 (2009).
- [13] R. Korlacki, A. Fukuda, J. K. Vij, A. Kocot, V. Görtz, M. Hird, and J. W. Goodby, *Phys. Rev. E* **72**, 041704 (2005).
- [14] PQS version 3.3, Parallel Quantum Solutions, 2013 Green Acres Road, Fayetteville, Arkansas 72703.
- [15] A. D. Becke, *J. Chem. Phys.* **98**, 1372 (1993).
- [16] C. Lee, W. Yang, and R. G. Parr, *Phys. Rev. B* **37**, 785 (1988).
- [17] W. J. Hehre, R. Ditchfield, and J. A. Pople, *J. Chem. Phys.* **56**, 2257 (1972).
- [18] P. C. Hariharan and J. A. Pople, *Theor. Chim. Acta* **28**, 213 (1973).
- [19] T. Clark, J. Chandrasekhar, G. W. Spitznagel, and P. R. Schleyer, *J. Comput. Chem.* **4**, 294 (1983).
- [20] P. Pulay, G. Fogarasi, G. Pongor, J. E. Boggs, and A. Vargha, *J. Am. Chem. Soc.* **105**, 7037 (1983).
- [21] J. Baker, A. A. Jarzecki, and P. Pulay, *J. Phys. Chem. A* **102**, 1412 (1998).
- [22] SQM, Parallel Quantum Solutions, 2013 Green Acres Road, Fayetteville, Arkansas 72703.
- [23] D. Dunmur and K. Toriyama, in *Handbook of Liquid Crystals*, edited by D. Demus, J. W. Goodby, G. W. Gray, H. Spiess, and V. Vill (Wiley-VCH, Weinheim, 1998), Vol. 1, p. 189.
- [24] M. D. Ossowska-Chruściel, R. Korlacki, A. Kocot, R. Wrzalik, J. Chruściel, and S. Zalewski, *Phys. Rev. E* **70**, 041705 (2004).
- [25] N. Hayashi and T. Kato, *Phys. Rev. E* **63**, 021706 (2001).
- [26] S. T. Lagerwall, P. Rudquist, and F. Giesselmann, *Mol. Cryst. Liq. Cryst.* **510**, 148 (2009).
- [27] J. P. F. Lagerwall, F. Giesselmann, and M. D. Radcliffe, *Phys. Rev. E* **66**, 031703 (2002).
- [28] R. Korlacki, A. Fukuda, and J. K. Vij, *EPL* **77**, 36004 (2007).
- [29] A. J. Leadbetter and E. K. Norris, *Mol. Phys.* **38**, 669 (1979).
- [30] C.-D. Poon and B. M. Fung, *Liq. Cryst.* **5**, 1159 (1989).
- [31] G. R. Luckhurst, C. Zannoni, P. L. Nordio, and U. Segre, *Mol. Phys.* **30**, 1345 (1975).
- [32] J. W. Emsley, R. Hashim, G. R. Luckhurst, G. N. Rumbles, and F. R. Vioria, *Mol. Phys.* **49**, 1321 (1983).
- [33] K. H. Kim, K. Ishikawa, H. Takezoe, and A. Fukuda, *Phys. Rev. E* **51**, 2166 (1995).
- [34] J. Matsushima, Y. Takanishi, K. Ishikawa, H. Takezoe, A. Fukuda, C. S. Park, W. G. Jang, K. H. Kim, J. E. MacLennan, M. A. Glaser, N. A. Clark, and K. Takahashi, *Liq. Cryst.* **29**, 27 (2002).
- [35] H. F. Gleeson, Y. Wang, S. Watson, D. Sahagun-Sanchez, J. W. Goodby, M. Hird, A. Petrenko, and M. A. Osipov, *J. Mater. Chem.* **14**, 1480 (2004).
- [36] M. V. Gorkunov and M. A. Osipov, *J. Phys. A: Math. Theor.* **41**, 295001 (2008).
- [37] R. Korlacki (unpublished).
- [38] W. L. McMillan, *Phys. Rev. A* **4**, 1238 (1971).
- [39] P. J. Wojtowicz, in *Introduction to Liquid Crystals*, edited by E. B. Priestley, P. J. Wojtowicz, and P. Sheng (Plenum Press, New York, 1975), p. 83.